ACS OMEGA

Article

Cite This: ACS Omega 2017, 2, 6741-6754

http://pubs.acs.org/journal/acsodf

Heterodimerization of Dibenzodiazepinone-Type Muscarinic Acetylcholine Receptor Ligands Leads to Increased M_2R Affinity and Selectivity

Xueke She,[†,§] Andrea Pegoli,[†] Judith Mayr,[†,∥] Harald Hübner,[‡] Günther Bernhardt,[†] Peter Gmeiner,[‡] and Max Keller*,[†]

[†]Institute of Pharmacy, Faculty of Chemistry and Pharmacy, University of Regensburg, Universitätsstr. 31, D-93053 Regensburg, Germany

[‡]Department of Chemistry and Pharmacy, Emil Fischer Center, Friedrich Alexander University, Schuhstr. 19, D-91052 Erlangen, Germany

Supporting Information

ABSTRACT: In search for selective ligands for the muscarinic acetylcholine receptor (MR) subtype M_2, the dimeric ligand approach, that is combining two pharmacophores in one and the same molecule, was pursued. Different types (agonists, antagonists, orthosteric, and allosteric) of monomeric MR ligands were combined by various linkers with a dibenzodiazepinone-type MR antagonist, affording five types of heterodimeric compounds ("DIBA-xanomeline," "DIBA-TBPB," "DIBA-77-LH-28-1," "DIBA-propantheline," and "DIBA-4-DAMP"), which showed high M_2R affinities (pK_i > 8.3). The heterodimeric ligand UR-SK75 (**46**) exhibited the highest M_2R affinity and selectivity [pK_i (M_1R–M_5R): 8.84, 10.14, 7.88, 8.59, and 7.47]. Two tritium-labeled dimeric derivatives ("DIBA-xanomeline"-type: [^{3}H]UR-SK71 ([^{3}H]**44**) and "DIBA-TBPB"-type: [^{3}H]UR-SK59 ([^{3}H]**64**)) were prepared to investigate their binding modes at hM_2R. Saturation-binding experiments showed that these compounds address the orthosteric binding site of the M_2R. The investigation of the effect of various allosteric MR modulators [gallamine (**13**), W84 (**14**), and LY2119620 (**15**)] on the equilibrium (**13**–**15**) or saturation (**14**) binding of [^{3}H]**64** suggested a competitive mechanism between [^{3}H]**64** and the investigated allosteric ligands, and consequently a dualsteric binding mode of **64** at the M_2R.

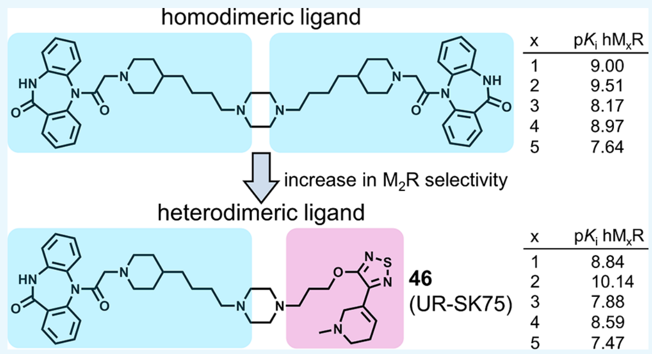

1. INTRODUCTION

Muscarinic acetylcholine receptors (MRs) belong to the class A G-protein coupled receptor (GPCR) superfamily and comprise five receptor subtypes in humans (designated M_1R–M_5R).[1−4] Whereas the M_1R, M_3R, and M_5R receptors were reported to couple with G_q proteins, the M_2R and M_4R receptors bind to $G_{i/o}$ proteins.[5] MRs represent interesting drug targets, for instance, for the treatment of Alzheimer's disease and schizophrenia.[6,7] Because of the high conservation of the orthosteric (acetylcholine) binding site,[8−10] there is lack of highly subtype selective (orthosteric) ligands, hampering therapeutic approaches such as the treatment of cognitive decline by centrally acting selective M_1R agonists or M_2R antagonists.[11] However, in addition to the orthosteric binding pocket, MRs were reported to exhibit distinct allosteric binding sites, which are less conserved and can potentially be exploited to develop subtype selective ligands.[12−17] The M_2R was the first GPCR described to be subjected to allosteric modulation,[18−20] and several dualsteric M_2R ligands (e.g., **7**[21] and **10**,[22,23] Figure 1A) and allosteric M_2R modulators (e.g., **13**,[20] **14**,[18] and **15**,[24,25] Figure 1B) were identified.

Dimerization of GPCR ligands can result in an increased receptor affinity and improved selectivity.[26,27] Bivalent (dimeric) ligands were described for various GPCRs, such as opioid,[28] histamine,[29,30] dopamine,[31−33] adenosine,[33−35] and neuropeptide Y[36−38] receptors, not least to investigate receptor dimerization. Likewise, the design of dualsteric (bitopic) ligands, that is, hybrid derivatives that simultaneously address the orthosteric and allosteric sites of one and the same receptor protomer, represents an approach toward improved subtype selectivity.[19,39−42] For example, rationally designed hybrid MR ligands derived from the orthosteric agonist oxotremorine (**2**) and hexamethonium-like allosteric modulators (e.g., compound **16**, Figure 1C) showed increased subtype selectivity compared to **2**.[43] Similarly, the MR ligand THRX-160209 (compound **17**, Figure 1C) was reported to exhibit a higher M_2R affinity and selectivity than the corresponding monovalent ligands and

Received: July 28, 2017
Accepted: September 5, 2017
Published: October 16, 2017

DOI: 10.1021/acsomega.7b01085
ACS Omega 2017, 2, 6741–6754

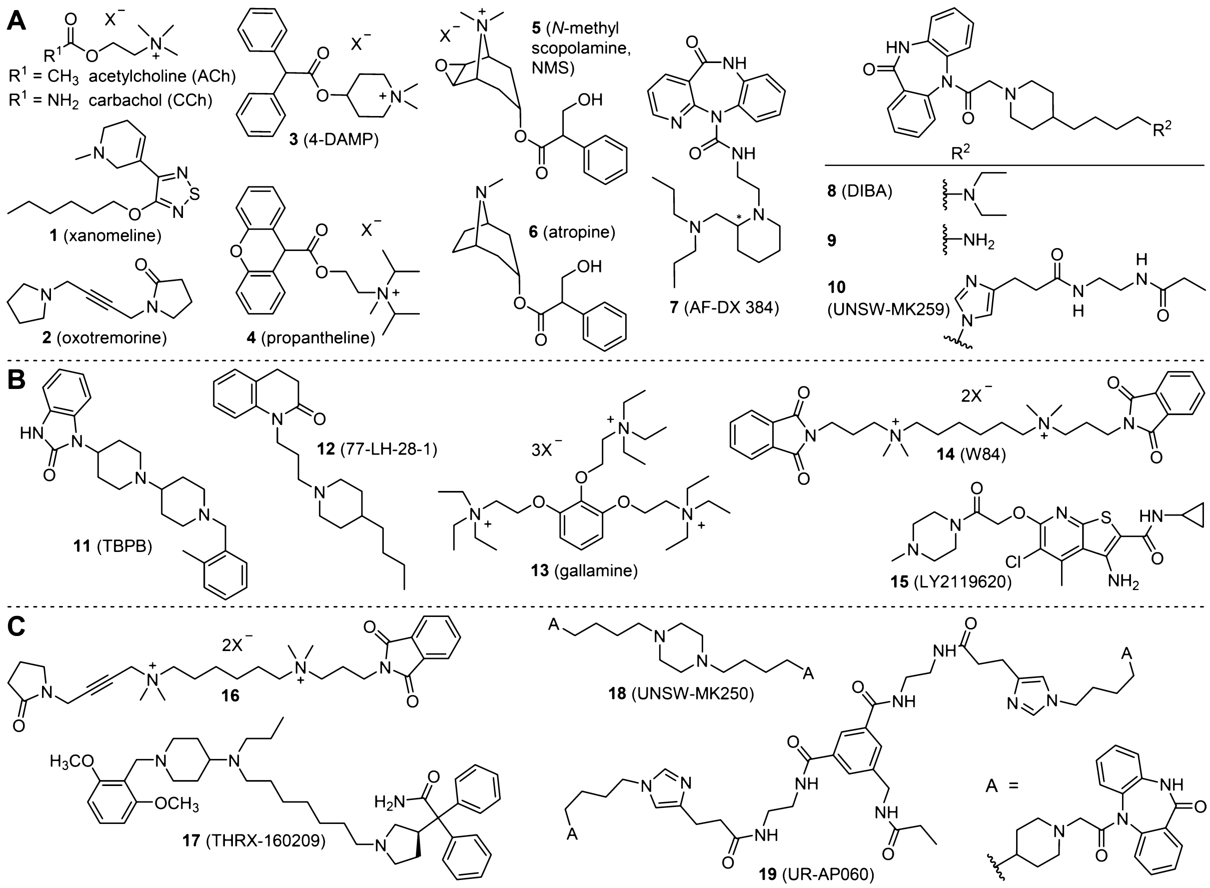

Figure 1. (A) Structures of the described MR agonists (ACh, CCh, **1**, and **2**) and antagonists (**3**−**10**). The M_2R binding poses of compounds **7** and **10** were reported to overlap in part with the binding pose of allosteric M_2R modulator **14**.[21,23] (B) Structures of the selected allosteric MR ligands (compounds **11**−**15**). (C) Structures of heterodimeric ligands **16** and **17** as well as homodimeric MR ligands **18** and **19**, the latter suggested to exhibit a dualsteric binding mode at the M_2R.[23]

was suggested to bind to the M_2 receptor in a multivalent manner.[44]

Pyridobenzodiazepinone derivative **7** and the structurally closely related dibenzodiazepinone derivative **8** (Figure 1A) represent tricyclic M_2R-preferring MR antagonists.[45,46] Tränkle et al. suggested a dualsteric binding mode of **7** at the M_2 receptor,[21] and a hybrid ligand formed of **7** and allosteric modulator **14** was reported to show a pronounced positive cooperativity with **5**, pointing at a new way for the development of allosteric enhancers.[47,48]

This study was aimed at the design, synthesis, and pharmacological evaluation of heterodimeric MR ligands derived from **8**, comprising five combinations of **8** with reported orthosteric or allosteric MR ligands: "**8**−xanomeline (**1**)," "**8**−TBPB (**11**)," "**8**−77-LH-28-1 (**12**)," "**8**−4-DAMP (**3**)," and "**8**−propantheline (**4**)." Xanomeline (**1**) (cf. Figure 1A) is a M_1 and M_4 receptor preferring MR agonist.[49] Compound **11** (cf. Figure 1B) was reported to selectively activate M_1 receptors through an allosteric mechanism, as shown by mutagenesis and molecular pharmacology studies;[50−52] in other reports, **11** was described as a bitopic M_1R ligand.[53] Likewise, compound **12** (cf. Figure 1B) was suggested to be a bitopic M_1R ligand.[54] MR antagonists **3** and **4** (cf. Figure 1A) are nonselective orthosteric MR antagonists with high affinities [K_i (**3**, M_1R−M_5R): 0.52−3.80 nM and K_i (**4**, M_1R−M_4R): 0.057−0.33 nM].[45,55] In addition to the heterodimeric ligands, one monomeric and four homodimeric ligands derived from xanomeline, one monomeric and two homodimeric ligands derived from **8**, and a monomeric ligand derived from **11** were prepared as reference compounds. Furthermore, two radiolabeled heterodimeric ligands (types "**8**−**11**" and "**8**−**1**") were prepared and characterized by saturation binding [including experiments in the presence of allosteric modulators (Schild-like analysis)], kinetic investigations, and competition-binding studies.

2. RESULTS AND DISCUSSION

2.1. Chemistry. Monomeric reference compound **22** and homodimeric xanomeline-derived ligand **25** were prepared by N-alkylation of homopiperazine derivative **21** using bromide **20** [followed by removal of the *tert*-butoxycarbonyl (Boc) group] and by alkylation of piperazine (**24**) using bromide **23**, respectively (Scheme 1). Treatment of amine **26** with octanedioyl dichloride or decanedioyl dichloride in the presence of triethylamine yielded homodimeric xanomeline-type compounds **27** and **28**, respectively. Likewise, amidation of terephthalic acid with amine **26**, using 1-ethyl-3-(3-dimethylaminopropyl)carbodiimide (EDC)/1-hydroxybenzotriazole hydrate (HOBt) as coupling reagent, afforded homodimeric ligand **29** containing a rigid central linker moiety. N-alkylation of **21** using bromide **30**, followed by removal of the Boc group, afforded TBPB derivative **31** (Scheme 1).

The "**8**−**11**" type heterodimeric ligand **34** was prepared by N-alkylation of compound **32** using bromide **33**; N-alkylation

DOI: 10.1021/acsomega.7b01085
ACS Omega 2017, 2, 6741−6754

Scheme 1. Synthesis of Xanomeline Derivatives 22, 25, and 27–29 as well as TBPB Derivative 31[a]

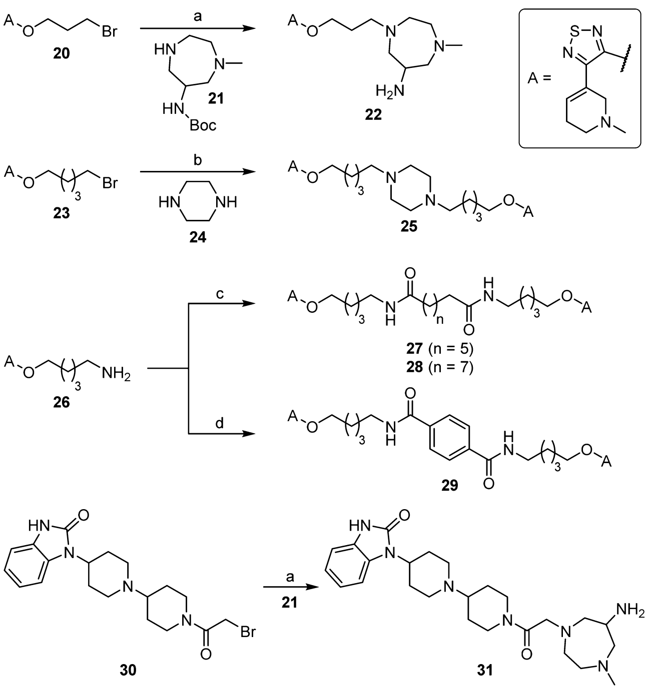

[a]Reagents and conditions: (a) (1) K_2CO_3, MeCN, microwave 110 °C, 30 min; (2) trifluoroacetic acid (TFA)/CH_2Cl_2 1:4 v/v, room temperature (rt), 8 h, 66% (**22**), 20% (**31**); (b) K_2CO_3, MeCN, microwave 110 °C, 30 min, 22%; (c) octanedioyl dichloride or decanedioyl dichloride, triethylamine, tetrahydrofuran (THF), 0 °C/rt, overnight, 39% (**27**), 65% (**28**); (d) terephthalic acid, EDC, HOBt, dimethylformamide (DMF), rt, overnight, 26%.

of **21** using **33**, followed by removal of the Boc group yielded monomeric reference compound **35** (Scheme 2). Likewise, N-alkylation of piperazine derivatives **36** and **37**, using bromide **33**, gave the "**8–4**" type heterodimeric ligands **38** and **39**. The "**8–1**" type heterodimeric ligand **43** was prepared through N-alkylation of compound **40** by applying a mixture of bromides **20** and **33**, followed by Boc-deprotection (Scheme 2). Homodimeric ligand **41**,[23] obtained as a "byproduct" (after Boc-deprotection), was isolated as well. Compound **41** was recently used as an amine precursor for the preparation of a tritium-labeled homodimeric MR ligand.[23] Amine **43** was propionylated to give congener **44**. The "**8–1**" type ligand **46** was obtained by N-alkylation of **45** by bromide **33** (Scheme 2). The "**8–3**" type heterodimeric ligand **48** and the "**8–12**" type ligand **50** were synthesized by alkylation of compound **47** using bromide **33** and by alkylation of amine **9**[22] (cf. Figure 1A) using bromide **49**, respectively (Scheme 2). Treatment of **40** with a mixture of bromides **30** and **33**, followed by Boc-deprotection, gave the "**8–11**" type heterodimeric ligand **51**, which contains a rigid homopiperazine moiety in between the pharmacophores. As in the case of the synthesis of **43**, homodimeric "byproduct" **41** was isolated. Propionylation of **51** gave congener **52** (Scheme 2). Homodimeric ligand **54** was obtained by treating an excess of compound **47** with bromide **53** (Scheme 2). Regarding the syntheses of **43** and **51**, it should be mentioned that the respective non-DIBA type homodimeric ligands, resulting from a double alkylation of **40** with bromides **20** or **30**, were formed as well, but were not isolated because of interference with other impurities [preparative high-performance liquid chromatography (HPLC)].

Amidation of isophthalic acid derivative **57** by applying a mixture of amines **55** and **56**, followed by Boc-deprotection, afforded heterodimeric ligand **60** and homodimeric ligand **58** (Scheme 3). Propionylation of **58** and **60** gave congeners **59** and **61**, respectively. By analogy, heterodimeric ligands **63**, **66**, **69**, and **72** were obtained by amidation of **57** using the amine mixtures **55**/**62**, **55**/**65**, **55**/**68**, and **55**/**71**, respectively, and subsequent Boc-deprotection (Scheme 3). Propionylation of **63**, **66**, and **69** at the central linker moiety afforded propionamide congeners **64**, **67**, and **70**. It should be noted that the respective non-DIBA type homodimeric ligands, generated by double amidation of **57** with amines **56**, **62**, **65**, **68**, or **71**, were formed but were not isolated (cf. Scheme 3).

2.2. Competition Binding at the Human MR Subtypes M_{1-5} with [^{3}H]N-Methylscopolamine ([^{3}H]5) as the Radioligand.

2.2.1. M_2R Affinity. M_2R receptor-binding affinities of monomeric reference ligands **22**, **31**, and **35**, homodimeric ligands **54** (type "**3–3**"), **58**, **59** (type "**8–8**"), and **25**, **27–29** (type "**1–1**"), as well as heterodimeric ligands **43**, **44**, **46**, **60**, and **61** (type "**8–1**"), **34**, **51**, **52**, **63**, and **64** (type "**8–11**"), **50** and **72** (type "**8–12**"), **38**, **39**, **69**, and **70** (type "**8–4**"), and **48**, **66**, and **67** (type "**8–3**") were determined at live CHO-hM_2R cells in equilibrium-binding experiments using the MR antagonist [^{3}H]**5** as the orthosterically binding radioligand. The results are summarized in Table 1.

All compounds containing a dibenzodiazepinone moiety showed high M_2R affinity (pK_i > 8.3). Whereas homodimeric derivatives (**25**, **27–29**) of MR agonist **1** exhibited an increased M_2R affinity (pK_i > 7.7) compared to the parent compound (pK_i of **1**: 6.55, see Table 3); the opposite was found in the case of MR antagonist **3** [pK_i = 7.09 ± 0.04, mean ± standard error of the mean (SEM) from two independent experiments] and a homodimeric derivative of **3** (compound **54**, pK_i = 6.05, Table 1). The "**8–1**" type heterodimeric ligand **46** displayed the highest M_2R affinity (pK_i = 10.14, Table 1). Steep curve slopes (≤−1.79) were observed for **43**, **51**, **60**, **61**, **64**, **67**, and **70**, indicating a complex mechanism of binding (e.g., the involvement of more than one binding site).

2.2.2. MR Receptor Subtype Selectivity. Selected dibenzodiazepinone-type heterodimeric ligands (**34**, **38**, **39**, **44**, **46**, **48**, **50**, **52**, **61**, **64**, **67**, **70**, and **72**) and monomeric dibenzodiazepinone derivative **35**, containing an amino-functionalized homopiperazine moiety, were also investigated by equilibrium competition binding at the MR subtypes M_1, M_3, M_4, and M_5 with [^{3}H]**5** as the radioligand (Table 1). For all compounds, there was a preference for the M_2R. Except for **38**, the M_1R and M_4R affinities were higher than the M_3R and M_5R affinities, that is, the selectivity profile was $M_2 > M_1 \approx M_4 > M_3/M_5$ (**34**, **39**, **44**, **46**, **48**, **50**, **52**, **61**, **64**, **67**, **70**, and **72**) and $M_2 > M_1 \approx M_5 > M_3 > M_4$ in the case of **38** (Table 1). Compound **46**, showing the highest M_2R affinity among the studied MR ligands, exhibited a more pronounced M_2R selectivity than the pyridobenzodiazepinone-type ligand **7** (cf. Figure 1A),[45] the MR antagonist tripitramine[56] containing three pyridobenzodiazepinone moieties, as well as the recently reported dibenzodiazepinone derivatives **10** and **19** (cf. Figure 1C).[23] Displacement of [^{3}H]**5** by **46** as well as by heterodimeric ligands **44** and **64**, which were prepared as tritiated ligands (see below), from M_xRs (determined at CHO-hM_xR cells, x = 1–5) is illustrated in Figure 2.

DOI: 10.1021/acsomega.7b01085
ACS Omega 2017, 2, 6741–6754

Scheme 2. Synthesis of DIBA (8)-Derived Heterodimeric Ligands 34, 38, 39, 43, 44, 46, 48, and 50−52, Monomeric Dibenzodiazepinone Derivative 35, and 4-DAMP (3)-Derived Homodimeric Ligand 54[a]

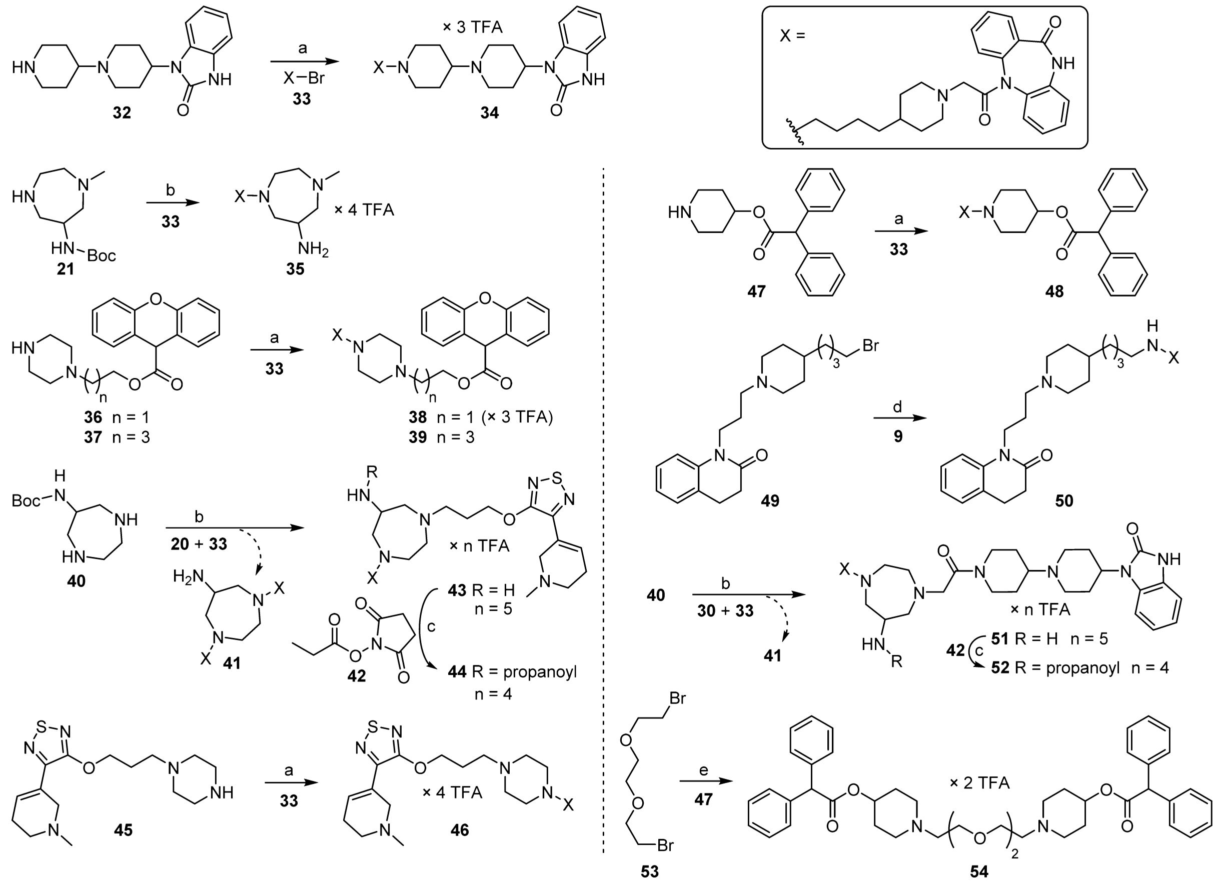

[a]Reagents and conditions: (a) K_2CO_3, MeCN, reflux, 3−6 h, 57% (**34**), 51% (**38**), 38% (**39**), 41% (**46**), 27% (**48**); (b) (1) K_2CO_3, MeCN, reflux (3 h or overnight) or microwave 110 °C (30 min); (2) TFA/CH_2Cl_2/H_2O 10:10:1 v/v/v, rt, 2 h, 12% (**35**), 17% (**43**), 12% (**51**); (c) diisopropylethylamine (DIPEA), DMF, rt, 2 h, 95% (**44**), 96% (**52**); (d) NaI, K_2CO_3, MeCN, reflux, 3 h, 52%; (e) K_2CO_3, MeCN, microwave 110 °C, 45 min, 23%.

2.3. Effect on IP1 Accumulation. As previously reported for homodimeric dibenzodiazepinone derivative **19**,[23] the homodimeric xanomeline-type ligand **25** and the heterodimeric dibenzodiazepinone-type ligands **44**, **46**, and **64** were investigated with respect to M_2R agonism and antagonism in an IP accumulation assay (Figure 3). Like **19**, compounds **44**, **46**, and **64** did not induce an IP1 accumulation when investigated in the agonist mode (Figure 3A), but completely suppressed the effect of CCh when studied in the antagonist mode (Figure 3B), revealing that the combination of the agonist xanomeline (**1**) with a dibenzodiazepinone-type antagonist in one molecule (e.g., **44**) resulted in a loss of agonistic activity. Interestingly, homodimeric ligand **25**, which is derived from MR agonist **1**, proved to be a M_2R antagonist in contrast to parent compound **1** (Figure 3). The pK_b values of **44**, **46**, and **64** (cf. Figure 3B) were lower compared to the respective pK_i values (cf. Table 1), as previously observed for homodimeric ligand **19**.[23] Possible reasons for this discrepancy are discussed elsewhere.[23]

2.4. Synthesis of the Radiolabeled Ligands [³H]44 and [³H]64. Aiming at a radiolabeled derivative of heterodimeric ligand **46**, which exhibited the highest M_2R affinity and selectivity (cf. Table 1), compound **44**, containing a propionamido-substituted homopiperazine moiety instead of the piperazine ring in **46** (cf. Scheme 2), was prepared as a tritiated derivative from amine precursor **43** and commercially available [^{3}H]**42** (Figure 4A). Additionally, the tritiated derivative of heterodimeric ligand **64** was prepared from **63** and [^{3}H]**42** (Figure 4A). The chemical stabilities of the "cold" analogues **44** and **64** were investigated under assaylike conditions [phosphate-buffered saline (PBS) pH 7.4] for over 48 h. **44** and **64** proved to be stable under these conditions (cf. SI Figure 1, Supporting Information). [^{3}H]**44** and [^{3}H]**64** were obtained in high radiochemical purities (98% and 99%, respectively; Figure 4B,D) and showed a high ([^{3}H]**44**) and excellent ([^{3}H]**64**) stability when stored in ethanol at −20 °C (cf. Figure 4C,E).

2.5. Characterization of [³H]44 and [³H]64. Saturation-binding experiments with [^{3}H]**44** and [^{3}H]**64** at intact CHO-hM_2R cells or CHO-hM_2R cell homogenates yielded monophasic saturation isotherms (Figure 5). As previously reported for [^{3}H]**19**,[23] the extent of unspecific binding strongly depended on the assay conditions: in the case of experiments performed at intact adherent cells (white/transparent 96-well plates), unspecific binding was considerably higher compared to experiments performed at cell homogenates, which preclude the unspecific binding of the radioligand to the microplate (Figure 5).[23] The apparent K_d values amounted to 1.0 and 0.081 nM (cell homogenates, Table 2). As orthosteric antagonist **6** (used to determine unspecific binding) completely

DOI: 10.1021/acsomega.7b01085
ACS Omega 2017, 2, 6741−6754

Scheme 3. Synthesis of Dibenzodiazepinone-Type Homo- or Heterodimeric Ligands 58−61, 63, 64, 66, 67, 69, 70, and 72[a]

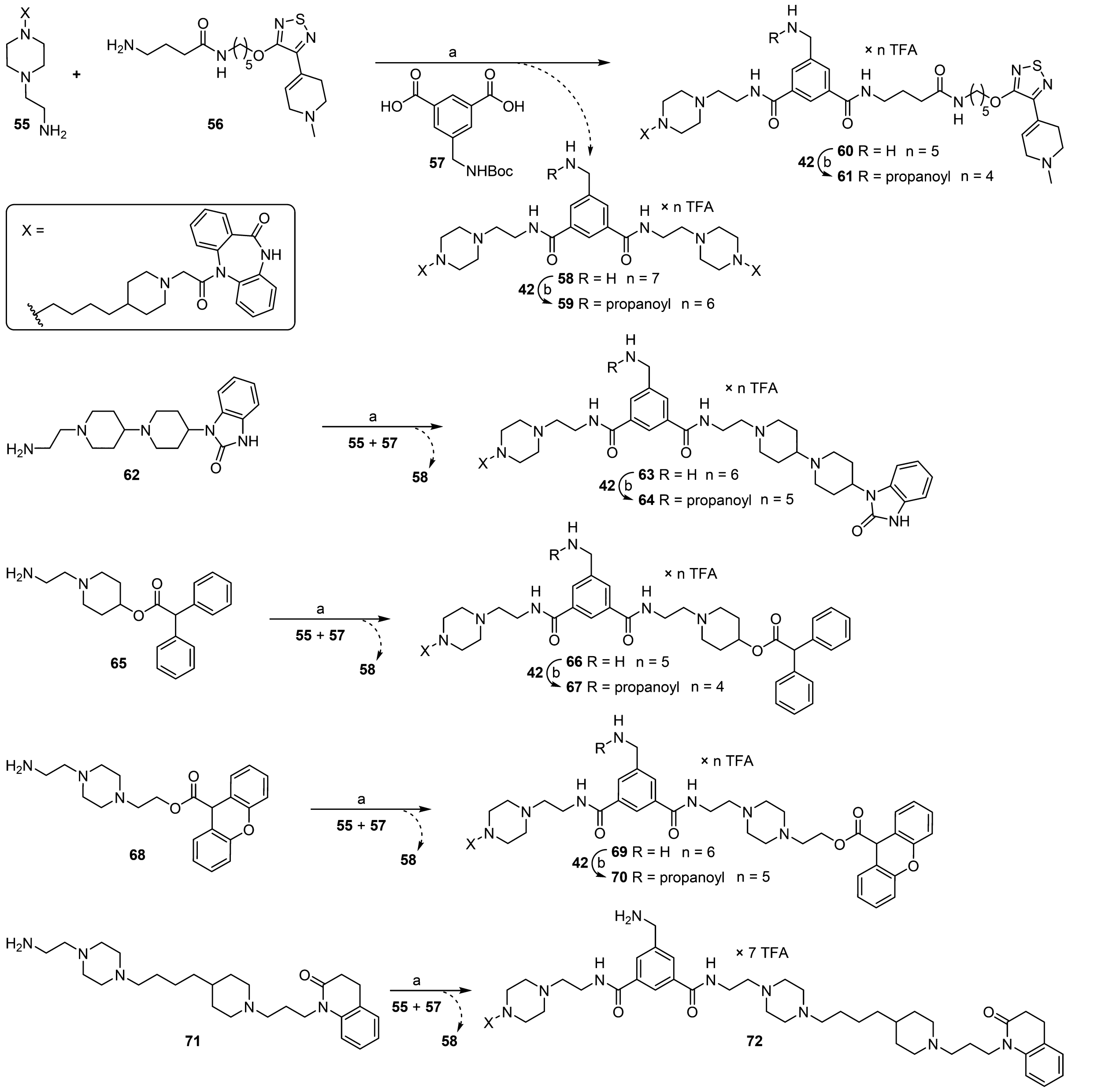

[a]Reagents and conditions: (a) (1) 2-(1*H*-benzotriazole-1-yl)-1,1,3,3-tetramethylaminium, HOBt, DIPEA, DMF, 60 °C, 3 h; (2) TFA/CH_2Cl_2/H_2O 10:10:1 v/v/v, rt, 2 h, 8% (**58**), 16% (**60**), 10% (**63**), 28% (**66**), 15% (**69**), 4% (**72**); (b) DIPEA, DMF, rt, 2 h, 79% (**59**), 89% (**61**), 88% (**64**), 83% (**67**), 86% (**70**).

prevented hyperbolic (monophasic) binding of the radioligands to the M_2R, these experiments proved that [^{3}H]**44** and [^{3}H]**64** bind to the orthosteric binding site of the M_2R, as previously reported for [^{3}H]**19**.[23]

The association of [^{3}H]**44** and [^{3}H]**64** with the human M_2R was monophasic and yielded similar k_{on} values (Figure 6A,C, Table 2). Whereas the "**8−1**" type heterodimeric ligand [^{3}H]**44** dissociated completely from the M_2R ($t_{1/2}$ = 47 min, cf. Figure 6B, Table 2), the dissociation of the "**8−11**" type dimeric ligand [^{3}H]**64** was incomplete, reaching a plateau at approximately 47% of initially M_2R-bound [^{3}H]**64** ($t_{1/2}$ = 35 min, cf. Figure 6D, Table 2). An incomplete ligand dissociation, which might be attributed to conformational adjustments of the receptor upon ligand binding[57] or an enhanced rebinding capability of the dimeric ligand,[58] was also reported for the homodimeric dibenzodiazepinone-type ligand [^{3}H]**19**.[23] The kinetically derived dissociation constants of both [^{3}H]**44** and [^{3}H]**64** [K_d(kin): 0.33 and 0.057 nM, respectively] were in good accordance with the K_d values obtained from the saturation-binding experiments (Table 2).

2.6. Competition Binding at the M_2R Using [^{3}H]44 and [^{3}H]64 as Radioligands.

Heterodimeric radioligands [^{3}H]**44** and [^{3}H]**64** were applied to equilibrium competition-binding experiments at CHO-hM_2R cell homogenates involving various reported orthosteric, dualsteric, and allosteric MR ligands. Orthosteric MR antagonist **6**, dualsteric ligand **10**, and allosteric modulator **14** (cf. Figure 1) were capable of totally displacing [^{3}H]**44** from the M_2R (SI Figure 2A, Supporting Information), indicating either a competitive mechanism or a strongly negative cooperativity between dimeric ligand [^{3}H]**44** and **6**,

Table 1. MR Affinities (pK_i Values) of Monomeric Reference Compounds 22, 31, and 35, Homodimeric Ligands 25, 27–29, 54, 58, and 59, as well as Heterodimeric Ligands 34, 38, 39, 43, 44, 46, 48, 50–52, 60, 61, 63, 64, 66, 67, 69, 70, and 72 Obtained from Equilibrium Competition-Binding Studies with [^{3}H]5 at Live CHO-hM$_x$R Cells (x = 1–5)

	M_1R		M_2R		M_3R		M_4R		M_5R	
Cmpd.	pK_i	slope[a]	pK_i	slope[a]	pK_i	slope[a]	pK_i	slope[a]	pK_i	slope[a]
22	n.d.	n.d.	4.90 ± 0.16	−1.01 ± 0.10	n.d.	n.d.	n.d.	n.d.	n.d.	n.d
25	7.36 ± 0.10	−1.04 ± 0.07	7.75 ± 0.18	−0.92 ± 0.18	7.30 ± 0.02	−0.95 ± 0.04	n.d.	n.d.	n.d.	n.d.
27	8.30 ± 0.08	−0.89 ± 0.10	8.46 ± 0.17	−0.94 ± 0.08	8.14 ± 0.04	−1.14 ± 0.03	n.d.	n.d.	n.d.	n.d.
28	8.41 ± 0.05	−1.30 ± 0.05	8.67 ± 0.11	−0.84 ± 0.07	n.d.	n.d.	n.d.	n.d.	n.d.	n.d.
29	7.72 ± 0.13	−1.15 ± 0.18	8.38 ± 0.13	−0.83 ± 0.06	n.d.	n.d.	n.d.	n.d.	n.d.	n.d.
31	n.d.	n.d.	5.88 ± 0.29	−0.87 ± 0.05	n.d.	n.d.	n.d.	n.d.	n.d.	n.d.
34	8.57 ± 0.05	−1.13 ± 0.05	9.12 ± 0.05	−1.43 ± 0.20	7.01 ± 0.11	−1.12 ± 0.07	7.95 ± 0.50	−1.18 ± 0.06	7.09 ± 0.07	−1.09 ± 0.20
35	7.26 ± 0.10	0.92 ± 0.08	8.67 ± 0.03	−0.87 ± 0.09	6.25 ± 0.06	−0.93 ± 0.20	8.00 ± 0.01	−0.77 ± 0.02[b]	6.86 ± 0.17	−1.09 ± 0.15
38	8.47 ± 0.08	−1.03 ± 0.12	8.82 ± 0.14	−1.08 ± 0.22	8.12 ± 0.05	−1.36 ± 0.09	7.99 ± 0.28	−0.98 ± 0.12	8.47 ± 0.06	−1.17 ± 0.10
39	7.62 ± 0.19	−1.40 ± 0.30	8.37 ± 0.28	−1.51 ± 0.26	7.01 ± 0.10	−0.85 ± 0.04	7.52 ± 0.35	−1.25 ± 0.10	7.03 ± 0.03	−1.09 ± 0.18
43	8.35 ± 0.07	−1.47 ± 0.17	9.30 ± 0.05	−2.19 ± 0.06[b]	7.21 ± 0.04	−1.34 ± 0.16	n.d.	n.d.	n.d.	n.d.
44	8.39 ± 0.03	−1.05 ± 0.05	9.34 ± 0.03	−1.14 ± 0.07	6.84 ± 0.03	−0.93 ± 0.04	8.24 ± 0.08	−0.94 ± 0.06	7.00 ± 0.09	−1.21 ± 0.19
46	8.84 ± 0.11	−1.45 ± 0.02[b]	10.14 ± 0.11	−0.96 ± 0.05	7.88 ± 0.06	−1.17 ± 0.08	8.59 ± 0.05	−1.17 ± 0.04	7.47 ± 0.03	−1.07 ± 0.22
48	7.68 ± 0.12	−1.03 ± 0.22	8.66 ± 0.03	−1.24 ± 0.22	7.46 ± 0.12	−1.35 ± 0.06[b]	8.07 ± 0.19	−1.17 ± 0.11	7.27 ± 0.05	−1.11 ± 0.10
50	8.40 ± 0.08	−1.00 ± 0.05	9.24 ± 0.11	−1.38 ± 0.22	6.86 ± 0.04	−1.05 ± 0.09	8.48 ± 0.03	−1.4 ± 0.06	7.03 ± 0.07	−1.01 ± 0.25
51	8.37 ± 0.03	−1.47 ± 0.05[b]	9.16 ± 0.07	−1.86 ± 0.05[b]	7.23 ± 0.06	−1.05 ± 0.10	n.d.	n.d.	n.d.	n.d.
52	7.78 ± 0.08	−1.82 ± 0.19[b]	9.11 ± 0.10	−1.12 ± 0.15	6.23 ± 0.10	−1.01 ± 0.03	8.10 ± 0.11	−0.85 ± 0.07	6.88 ± 0.10	−1.31 ± 0.10
54	6.59 ± 0.07	−1.14 ± 0.12	6.05 ± 0.06	−1.33 ± 0.18	5.64 ± 0.09	−1.05 ± 0.34	5.63 ± 0.04	−1.00 ± 0.06	5.87 ± 0.25	−1.35 ± 0.20
58	8.69 ± 0.09	−2.06 ± 0.19[b]	9.83 ± 0.07	−1.53 ± 0.15	7.78 ± 0.05	−1.27 ± 0.10	n.d.	n.d.	n.d.	n.d.
59	8.53 ± 0.08	−1.75 ± 0.34	9.24 ± 0.06	−1.31 ± 0.09	7.89 ± 0.07	−1.22 ± 0.09	n.d.	n.d.	n.d.	n.d.
60	8.80 ± 0.10	−1.32 ± 0.31	9.65 ± 0.15	−1.79 ± 0.09[b]	7.76 ± 0.14	−1.28 ± 0.04[b]	n.d.	n.d.	n.d.	n.d.
61	8.88 ± 0.08	−1.61 ± 0.03[b]	9.47 ± 0.07	−2.37 ± 0.15[b]	7.87 ± 0.02	−0.99 ± 0.04	8.87 ± 0.08	−1.14 ± 0.11	8.37 ± 0.24	−1.02 ± 0.11
63	8.79 ± 0.09	−1.19 ± 0.07	9.71 ± 0.08	−1.37 ± 0.14	7.77 ± 0.03	−1.22 ± 0.05	n.d.	n.d.	n.d.	n.d.
64	8.56 ± 0.11	−1.59 ± 0.15	9.44 ± 0.06	−1.84 ± 0.17[b]	7.55 ± 0.04	−1.40 ± 0.10	8.57 ± 0.02	−1.01 ± 0.04	6.96 ± 0.04	−1.26 ± 0.14
66	8.28 ± 0.05	−1.32 ± 0.19	9.16 ± 0.20	−1.64 ± 0.23	7.20 ± 0.19	−1.33 ± 0.08	n.d.	n.d.	n.d.	n.d.
67	8.38 ± 0.06	−1.54 ± 0.14	8.94 ± 0.07	−2.14 ± 0.16[b]	7.52 ± 0.04	−1.25 ± 0.09	8.50 ± 0.08	−1.52 ± 0.26	7.62 ± 0.06	−1.51 ± 0.12
69	8.42 ± 0.19	−1.74 ± 0.19	9.17 ± 0.18	−1.52 ± 0.31	7.26 ± 0.22	−1.23 ± 0.12	n.d.	n.d.	n.d.	n.d.
70	8.51 ± 0.13	−1.10 ± 0.07	8.96 ± 0.08	−2.14 ± 0.18[b]	7.72 ± 0.06	−1.21 ± 0.13	8.29 ± 0.02	−1.41 ± 0.05[b]	7.37 ± 0.08	−1.01 ± 0.12
72	8.52 ± 0.09	−1.66 ± 0.20	9.63 ± 0.03	−1.31 ± 0.13	7.88 ± 0.03	−1.42 ± 0.09[b]	8.39 ± 0.09	−1.50 ± 0.17	7.69 ± 0.33	−0.85 ± 0.07

[a]Curve slope of the four-parameter logistic fit. Presented are mean values ± SEM from three to five independent experiments (each performed in triplicate). K_d values reported previously[22]/applied concentrations of [^{3}H]**5**: M_1: 0.12/0.2 nM; M_2: 0.090/0.2 nM; M_3: 0.0895/0.2 nM; M_4: 0.040/0.1 nM; and M_5: 0.24/0.3 nM. [b]Slope different from unity (P < 0.05).

DOI: 10.1021/acsomega.7b01085
ACS Omega 2017, 2, 6741–6754

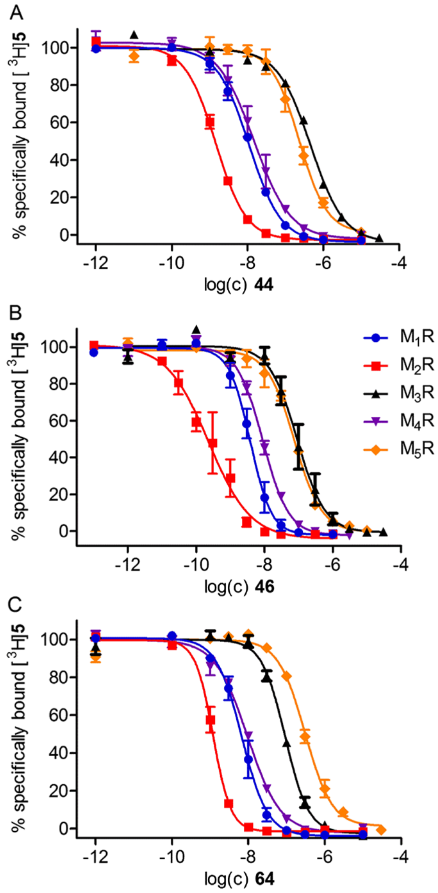

Figure 2. Displacement of $[^3H]$**5** [c = 0.2 nM (M_1, M_2, M_3), 0.1 nM (M_4), or 0.3 nM (M_5)] by heterodimeric ligands **44** (A), **46** (B), and **64** (C) from M_xRs determined at intact CHO-hM_xR cells (x = 1−5). Data represent mean values ± SEM from at least three independent experiments (performed in triplicate).

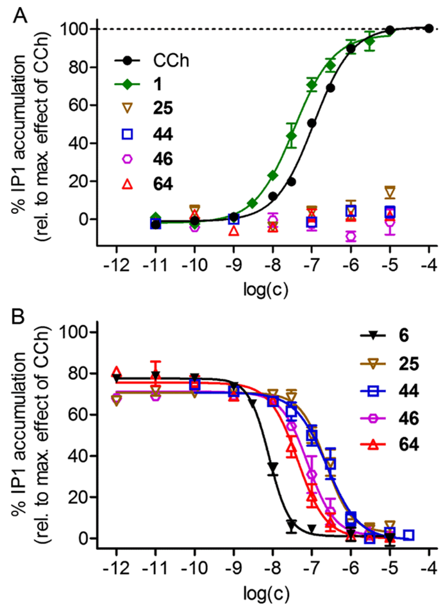

Figure 3. M_2R agonism and antagonism of **25**, **44**, **46**, and **64** investigated in an IP1 accumulation assay using HEK-hM_2-G$\alpha q_{i5\text{-}HA}$ cells. (A) Concentration-dependent effect of CCh, **1**, **25**, **44**, **46**, and **64** on the accumulation of IP1. **25**, **44**, **46**, and **64** elicited no response. pEC_{50} of CCh and **1**:6.96 and 7.45, respectively. Data represent mean values ± SEM from at least seven (CCh and **1**) or at least two (**25**, **44**, **46**, and **64**) independent experiments (each performed in triplicate). (B) Concentration-dependent inhibition of the IP1 accumulation induced by CCh (0.3 μM) by **6**, **25**, **44**, **46**, and **64**. Corresponding pK_b values: **6**: 8.63,[23] **25**: 7.21, **44**: 7.18, **46**: 7.67, and **64**: 7.93. Data represent mean values ± SEM from at least five independent experiments (each performed in duplicate).

10, or **14**. Likewise, orthosteric ligands **1** and **6**, dualsteric ligands **7** and **10**, as well as allosteric modulators **13**−**15** (cf. Figure 1) completely displaced $[^3H]$**64** from the M_2R-specific binding sites. (SI Figure 2B, Supporting Information). For most of the investigated MR ligands, the respective pK_i values were in good agreement with the binding data obtained from competition binding with $[^3H]$**5** (Table 3). However, the pK_i values of compounds **1**, **6**, **7**, and **10**, determined in the presence of $[^3H]$**64**, were consistently lower (up to 1 log unit in the case of **7**) than pK_i values from the competition-binding experiments with $[^3H]$**5**. This is in agreement with the (in part) irreversible M_2R binding of $[^3H]$**64** (cf. Figure 6D), which compromises its use as a molecular tool for the determination of binding constants of nonlabeled ligands, as was also reported for homodimeric MR ligand $[^3H]$**19**.[23]

2.7. Schild-like Analysis with $[^3H]$64 and Allosteric M_2R Modulator 14. To further explore the binding mode of heterodimeric ligand **64** at the M_2R, saturation-binding experiments were performed with $[^3H]$**64** in the presence of increasing concentrations of allosteric M_2R ligand **14** (Figure 7), as recently reported for homodimeric radioligand $[^3H]$**19**.[23] As in the case of $[^3H]$**19**,[23] this Schild-like analysis resulted in rightward-shifted saturation isotherms of $[^3H]$**64** (Figure 7A) and a linear Schild plot with a slope not different from unity (Figure 7B), which is consistent with a competitive mechanism between $[^3H]$**64** and allosteric M_2R ligand **14**. With regard to the fact that $[^3H]$**64** binds to the orthosteric binding site of the M_2R (see above), these results strongly support a dualsteric binding mode of **64** at the human M_2R. The "pA_2" value of 7.16, obtained for **14** from the Schild regression (Figure 7B), was in accordance with the reported M_2R binding data of **14** (pK_X 7.50[59]).

3. CONCLUSIONS

Linking orthosteric (**1**, **3**, and **4**) and allosteric (**11** and **12**) MR ligands with a M_2R preferring dibenzodiazepinone-type MR antagonist (**8**) yielded a series of heterodimeric ligands (**34**, **38**, **39**, **43**, **44**, **46**, **48**, **50**−**52**, **60**, **61**, **63**, **64**, **66**, **67**, **69**, **70**, and **72**). The "8−1" type dimeric ligand **46** (UR-SK75), containing a piperazine moiety in the linker, exhibited a higher M_2R affinity (pK_i 10.14) and selectivity [expressed as the ratio of K_i values (M_1/M_2/M_3/M_4/M_5): 23:1:180:29:430] compared to monomeric (such as **8**[46] and **10**[22,23]) and homodimeric (e.g., **18**[22] and **19**[23]) dibenzodiazepinone-type ligands. High M_2R affinity of all dibenzodiazepinone-type heterodimeric ligands (pK_i > 8.3, Table 1), as also reported for monomeric dibenzodiazepinone-type ligands,[22] suggested a minor influence of the second pharmacophore on M_2R binding, indicating that the high M_2R affinity of these compounds is mediated by the "dibenzodiazepinone" pharmacophore, which binds most likely to the orthosteric binding site of the M_2R. This is supported by the proposed binding mode of **10** and **19** at the M_2R,[23] by saturation-binding studies using the radioligands $[^3H]$**44** ($[^3H]$UR-SK71) and $[^3H]$**64** ($[^3H]$UR-SK59), and by the fact that compounds containing M_1R/M_4R selective agonist **1**[49]

DOI: 10.1021/acsomega.7b01085
ACS Omega 2017, 2, 6741−6754

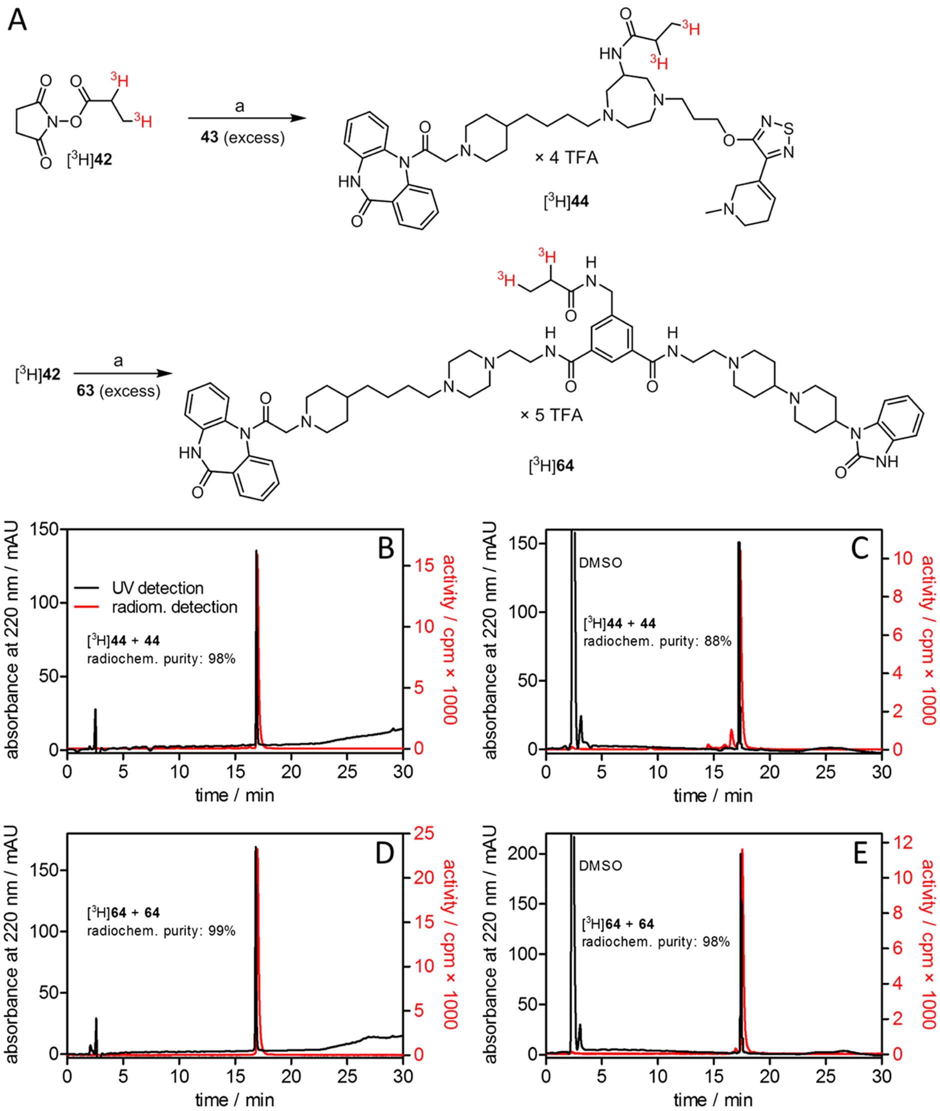

Figure 4. Preparation, purity, and identity control of the radiolabeled dibenzodiazepinone derivatives [^{3}H]**44** and [^{3}H]**64**. (A) Synthesis of [^{3}H]**44** and [^{3}H]**64** by [^{3}H]propionylation of amine precursors **43** and **63**, respectively, using succinimidyl [^{3}H]propionate ([^{3}H]**42**). Reagents and conditions: (a) DIPEA, DMF, rt, 1.5 h, radiochemical yields: 36% ([^{3}H]**44**) and 35% ([^{3}H]**64**). (B,C) HPLC analysis of [^{3}H]**44** (0.18 μM) spiked with "cold" **44** (3 μM), analyzed 3 days after synthesis (B) and after 10 months of storage at −20 °C in EtOH/H_2O (1:1) (C). (D,E) HPLC analysis of [^{3}H]**64** (0.23 μM) spiked with "cold" **64** (3 μM), analyzed 3 days after synthesis (D) and after 10 months of storage at −20 °C in EtOH/H_2O (1:1) (E). HPLC conditions are provided in the Supporting Information.

as a second pharmacophore (**43**, **44**, **46**, **60**, and **61**) proved to be M_2R-preferring ligands. Moreover, the prototypical heterodimeric ligands **44** and **46** were shown to be M_2R antagonists (cf. Figure 3). Concerning the "**8**−**1**" type heterodimeric ligands, one can speculate about the contribution of the pharmacophore of **1** to M_2R binding because the homodimeric derivatives of **1** (compounds **25**, **27**−**29**) exhibited considerably higher M_2R affinities compared to **1**. This work confirms that dibenzodiazepinone-type MR ligands represent a promising class of compounds for the development of highly selective M_2R ligands with a high receptor affinity based on the dualsteric ligand approach.

4. METHODS

4.1. General Experimental Conditions. Reagents and chemicals for synthesis were purchased from Acros Organics (Geel, Belgium), Iris Biotech (Marktredwitz, Germany), Alfa Aesar (Karlsruhe, Germany), Merck (Darmstadt, Germany), Sigma (Munich, Germany), or TCI Europe (Zwijndrecht, Belgium). Technical grade solvents (acetone, ethyl acetate, light petroleum (40−60 °C), and CH_2Cl_2) were distilled before use. Deuterated solvents for nuclear magnetic resonance (NMR) spectroscopy were from Deutero (Kastellaun, Germany). Acetonitrile for HPLC (gradient grade) was obtained from Merck or Sigma. Anhydrous DMF was purchased from Sigma. CCh (Sigma) and compounds **6** (Sigma), **7** (Abcam, Cambridge, UK), **13** (Sigma), **14** (Sigma), and **15** (Absource Diagnostic, Munich, Germany) were purchased from commercial suppliers. The radiolabeled MR antagonist [^{3}H]**5** (specific activity = 80 Ci/mmol) was purchased from American Radiolabeled Chemicals Inc. (St. Louis, MO) via Hartmann Analytic (Braunschweig, Germany). The syntheses of compounds **40**,[23] **42**,[60] and **57**[23] are described elsewhere. Compounds **1**,[61] **120**,[23] and **123**[62] were prepared according to described procedures.

DOI: 10.1021/acsomega.7b01085
ACS Omega 2017, 2, 6741−6754

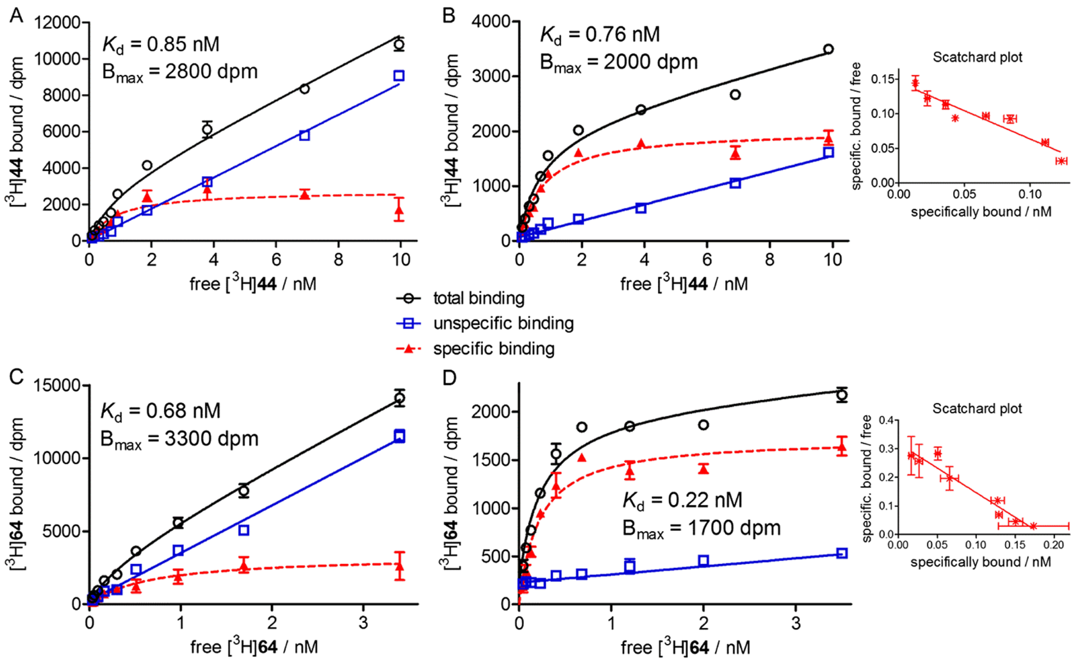

Figure 5. Representative hyperbolic (monophasic) isotherms of specific M_2R binding (red dashed line) of $[^3H]$**44** (A,B) and $[^3H]$**64** (C,D) obtained from saturation-binding experiments either performed with live adherent CHO-hM_2R cells (A,C) or CHO-hM_2R cell homogenates (B,D). Unspecific binding (blue solid line) was determined in the presence of MR antagonist **6** (500-fold excess). Experiments were performed in triplicate. The error bars of specific binding and error bars in the Scatchard plots represent propagated errors calculated according to the Gaussian law of errors. The error bars of total and unspecific binding represent the SEM.

Table 2. M_2R Binding Characteristics of $[^3H]$44 and $[^3H]$64

	saturation-binding	binding kinetics		
radioligand	K_d [nM][a]	K_d(kin) [nM][b]	k_{on} [min^{-1} nM^{-1}][c]	k_{off} [min^{-1}][d], $t_{1/2}$ [min][d]
$[^3H]$44	1.0 ± 0.2	0.20 ± 0.03	0.078 ± 0.015	0.015 ± 0.001, 47 ± 3
$[^3H]$64	0.081 ± 0.022	0.072 ± 0.002	0.31 ± 0.01	0.022 ± 0.002, 35 ± 1

[a]Dissociation constant determined by saturation binding at CHO-hM_2R cell homogenates; mean ± SEM from at least three independent experiments (performed in triplicate). [b]Kinetically derived dissociation constant ± propagated error [K_d(kin) = k_{off}/k_{on}]. [c]Association rate constant ± propagated error, calculated from k_{obs} (nonlinear regression), k_{off} (nonlinear regression), and the applied radioligand concentration (cf. Radioligand Binding). [d]Dissociation rate constant (nonlinear regression, two ($[^3H]$**44**)- or three ($[^3H]$**64**)-parameter equation describing a monophasic decline) and half-life; mean ± SEM from three independent experiments (performed in triplicate).

Millipore water was used throughout for the preparation of buffers and HPLC eluents. If moisture-free conditions were required, reactions were performed in dried glassware under an inert atmosphere (argon). Anhydrous THF was obtained by distillation over sodium, and anhydrous CH_2Cl_2 was prepared by distillation over P_2O_5 after predrying over $CaCl_2$. Reactions were monitored by thin-layer chromatography using aluminum plates coated with silica gel (Merck silica gel 60 F_{254}, thickness 0.2 mm). Spots were detected by ultraviolet (UV) light (254 or 366 nm) or by staining using 0.3% solution of ninhydrin in *n*-butanol (amines) or iodine. Column chromatography was performed in glass columns on silica gel (Merck silica gel 60, 63−200 μm). Flash chromatography was performed on an Intelli Flash-310 Flash-Chromatography Workstation (Varian, Darmstadt, Germany). Polypropylene reaction vessels (1.5 or 2 mL) with a screw cap (Süd-Laborbedarf, Gauting, Germany) were used for the synthesis of radioligands ($[^3H]$**44** and $[^3H]$**64**) for small-scale reactions, for the investigation of chemical stabilities (**44** and **64**), and for the preparation and storage of stock solutions. Melting points were measured with a Büchi 530 (Büchi, Essen, Germany) apparatus and are uncorrected. Microwave-assisted reactions were performed with an Initiator 2.0 synthesizer (Biotage, Uppsala, Sweden). NMR spectra were recorded on a Bruker AVANCE 300 (7.05 T), Bruker AVANCE III HD 400 (9.40 T), or a Bruker AVANCE III HD 600 spectrometer equipped with a cryogenic probe (14.1 T) (Bruker, Karlsruhe, Germany). Abbreviations for the multiplicities of the signals are s (singlet), d (doublet), t (triplet), dd (doublet-of-doublet), q (quartet), m (multiplet), and brs (broad-singlet). Infrared (IR) spectra were measured with a Nicolet 380 FT-IR spectrophotometer (Thermo Electron Corporation). Low-resolution mass spectrometry was performed on a Finnigan SSQ 710A instrument [chemical ionization mass spectrometry (CI-MS, Thermo Finnigan, San Jose, CA). High-resolution mass spectrometry (HRMS) analysis was performed on an Agilent 6540 UHD Accurate-Mass Q-TOF LC/MS system (Agilent Technologies, Santa Clara, CA) using an electrospray ionization source. Preparative HPLC was performed on a system from Knauer (Berlin, Germany) consisting of two K-1800 pumps and a K-2001 detector. Except for compound **54**, a Kinetex-XB C18 column, 5 μm, 250 × 21 mm (Phenomenex, Aschaffenburg, Germany) served as the stationary phase at a flow rate of 15 mL/min. For the purification of **54**, a Nucleodur 100-5 C18 column, 5 μm,

DOI: 10.1021/acsomega.7b01085
ACS Omega 2017, 2, 6741−6754

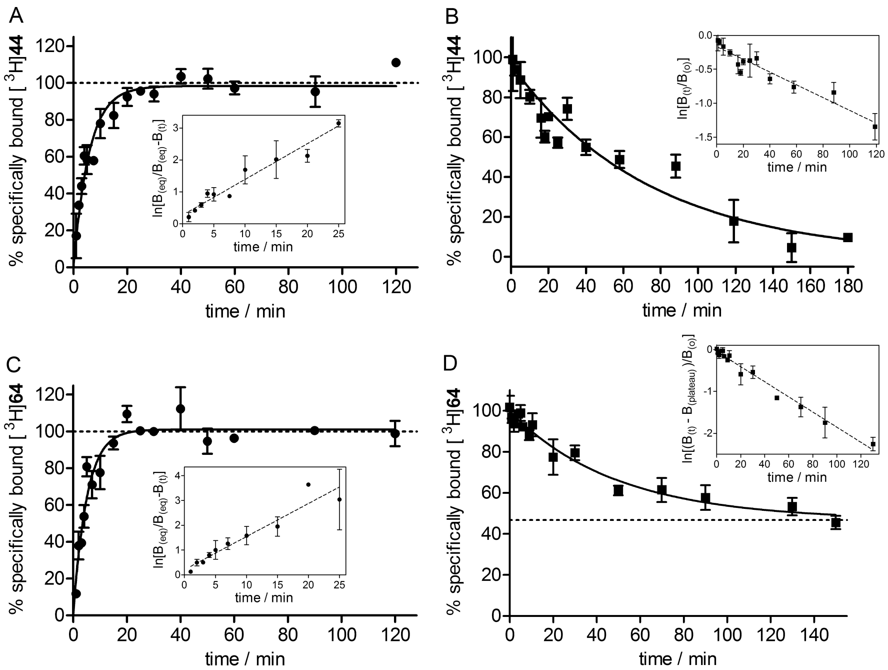

Figure 6. Association and dissociation kinetics of [^{3}H]**44** (A,B) and [^{3}H]**64** (C,D) determined at CHO-hM$_2$R cell homogenates at 23 °C. (A) Association of [^{3}H]**44** (c = 2 nM) with the M$_2$R. Inset: $\ln[B_{(eq)}/(B_{(eq)} - B_{(t)})]$ vs time. (B) Dissociation of [^{3}H]**44** (preincubation: 4 nM, 1 h) from the M$_2$R determined in the presence of **6** (1000-fold excess), showing complete monophasic exponential decline. Inset: $\ln[B_{(t)}/B_{(0)}]$ vs time. (C) Association of [^{3}H]**64** (c = 0.6 nM) with the M$_2$R. Inset: $\ln[B_{(eq)}/(B_{(eq)} - B_{(t)})]$ vs time. (D) Dissociation of [^{3}H]**64** (preincubation: 0.6 nM, 1 h) from the M$_2$R determined in the presence of **6** (1000-fold excess), showing incomplete monophasic exponential decline. Inset: $\ln[(B_{(t)} - B_{(plateau)})/B_{(0)}]$ versus time. For k_{on} and k_{off} values, see Table 2. Data represent mean ± SEM from three (A,B,D) or two (C) independent experiments (each performed in triplicate).

Table 3. M$_2$R Binding Data (pK_i or pIC$_{50}$ Values) of Various Orthosteric (1 and 6), Allosteric (13−15), Dualsteric (7 and 10) MR Ligands, and 64 Determined with [^{3}H]44, [^{3}H]64, or [^{3}H]5

ligand	[^{3}H]**44** pK_i[a]	[^{3}H]**64** pK_i[a]	[^{3}H]**5** pK_i* or pIC$_{50}$**[b]
1		5.78 ± 0.05	6.55 ± 0.05*
6	8.52 ± 0.26	8.52 ± 0.14	9.04 ± 0.08*
7		7.71 ± 0.14	8.71 ± 0.05*
10	9.61 ± 0.11	8.35 ± 0.09	9.11 ± 0.05*
13		5.60 ± 0.07	6.11 ± 0.09**[c]
14	5.90 ± 0.22	6.08 ± 0.28	6.32 ± 0.18**[c]
15		5.43 ± 0.02	<4.5**[c]
64		9.44 ± 0.01	9.44 ± 0.06*

[a]Determined by equilibrium competition binding with [^{3}H]**44** (2 nM) or [^{3}H]**64** (0.3 nM) at CHO-hM$_2$R cell homogenates; mean values ± SEM from at least three independent experiments (performed in triplicate). [b]Determined by equilibrium competition binding with [^{3}H]**5** (0.2 nM) at live CHO-hM$_2$R cells; mean ± SEM from at least three independent experiments (performed in triplicate). [c]Reported by Pegoli et al.[23]

250 × 21 mm (Macherey-Nagel, Düren, Germany) was used as the stationary phase at a flow rate of 15 mL/min. Mixtures of acetonitrile and 0.1% aq TFA were used as the mobile phase, and a detection wavelength of 220 nm was used throughout. Lyophilization of the collected fractions was performed with an Alpha 2-4 LD apparatus (Martin Christ, Osterode am Harz, Germany). Except for compound **54**, analytical HPLC analysis (purity control) was performed on a system from Merck-Hitachi (Hitachi, Düsseldorf, Germany) composed of a L-6200-A pump, an AS-2000A autosampler, a L-4000A UV detector, and a D-6000 interface. A Kinetex-XB C18 column, 5 μm, 250 mm × 4.6 mm (Phenomenex, Aschaffenburg, Germany) was used as the stationary phase at a flow rate of 0.8 mL/min. Mixtures of acetonitrile (A) and 0.1% aq TFA (B) were used as the mobile phase (degassed by helium purging). The following linear gradient was applied: 0−30 min: A/B 5:95−85:15, 30−32 min: 85:15−95:5, and 32−40 min: 95:5. Detection was performed at 220 nm throughout. The oven temperature was 30 °C. Analytical HPLC analysis of **54** was performed on a system from Thermo Separation Products composed of a SN400 controller, a P4000 pump, a degasser (Degassex DG-4400, Phenomenex), an AS3000 autosampler, and a Spectra Focus ultraviolet−visible detector. A Eurospher-100 C18 column, 5 μm, 250 × 4 mm (Knauer, Berlin, Germany) served as reversed-phase (RP) column at a flow rate of 0.8 mL/min. Mixtures of acetonitrile (A) and 0.05% aq TFA (B) were used as the mobile phase (degassed by helium purging). The oven temperature was set to 30 °C, and detection was performed at 220 nm. The following linear gradient was applied: 0−30 min: A/B 20:80−95:5 and 30−40 min: 95:5.

Annotation concerning the NMR spectra (^{1}H, ^{13}C) of the dibenzodiazepinone derivatives (**34**, **35**, **38**, **39**, **43**, **44**, **46**, **48**, **50**, **52**, **58**−**61**, **63**, **64**, **66**, **69**, and **72**): due to a slow rotation about the exocyclic amide group on the NMR time scale, two isomers (ratios provided in the experimental protocols) were evident in the ^{1}H- and ^{13}C-NMR spectra.

4.2. Compound Characterization. Nondescribed intermediate compounds were characterized by ^{1}H- and ^{13}C-NMR spectroscopy, HRMS, and melting point (if applicable). Target compounds were characterized by ^{1}H- and ^{13}C-NMR spectroscopy, HRMS, and RP-HPLC analysis. In addition, compounds **44** and **64** were analyzed by IR spectroscopy. Purities determined by analytical RP-HPLC amounted to >95%.

DOI: 10.1021/acsomega.7b01085
ACS Omega 2017, 2, 6741−6754

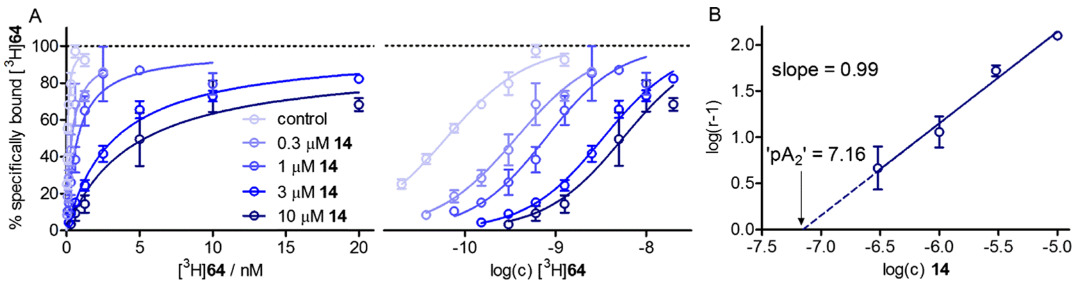

Figure 7. Effect of allosteric M_2R modulator **14** on the saturation binding of [^{3}H]**64** determined at CHO-hM_2R cell homogenates at 22 °C. (A) Isotherms of specific radioligand binding plotted in the linear and semilogarithmic scale. The presence of compound **14** led to a rightward shift of the saturation isotherms of [^{3}H]**64**. (B) "Schild" regression resulting from the rightward shifts (ΔpK_d) of the saturation isotherms [log($r - 1$) plotted vs log(concentration **14**), where $r = 10^{\Delta pK_d}$]. The slope of the linear Schild regression was not different from unity [$P > 0.5$, based on the slope mean value ± SEM (0.99 ± 0.15) from three sets of independent saturation-binding experiments (performed in triplicate)], suggesting a competitive interaction between [^{3}H]**64** and **14**. Data represent mean values ± SEM from three independent experiments (each performed in triplicate).

4.3. Investigation of the Chemical Stability. The chemical stability of **44** and **64** was investigated in PBS (pH 7.4) at 22 ± 1 °C. The incubation was started by addition of 10 mM solution of the compounds in dimethylsulfoxide (1 µL) to PBS (99 µL) to give a final concentration of 100 µM. After 0, 12, and 48 h, an aliquot (20 µL) of the solution was taken and added to acetonitrile/0.04% aq TFA (1:9 v/v) (20 µL). An aliquot (20 µL) of the resulting solution was analyzed by RP-HPLC using a system from Agilent Technologies (composed of a 1290 Infinity binary pump equipped with a degasser, a 1290 Infinity autosampler, a 1290 Infinity thermostated column compartment, a 1260 Infinity diode array detector, and a 1260 Infinity fluorescence detector). A Kinetex-XB C18 column, 2.6 µm, 100 × 3 mm (Phenomenex) served as the stationary phase at a flow rate of 0.5 mL/min. The following linear gradient was applied: 0−20 min: acetonitrile/0.04% aq TFA 10:90−68:32, 20−22 min: 68:32−95:5, and 22−28 min: 95:5. The detection wavelength was set to 220 nm.

4.4. Cell Culture and Preparation of Cell Homogenates. The culture conditions of CHO-K9 cells, stably transfected with the human muscarinic receptors M_1−M_5 (obtained from Missouri S&T cDNA Resource Center; Rolla, MO), and the preparation of CHO-hM_2R cell homogenates are described elsewhere.[23]

4.5. IP1 Accumulation Assay. The IP1 accumulation assay was performed as described elsewhere.[23]

4.6. Radioligand Binding. Equilibrium competition-binding experiments with [^{3}H]**5** were performed at intact CHO-hM_xR cells (x = 1−5) as described previously,[22] but the total volume per well was 200 µL, that is, in the case of total binding, the wells were filled with 180 µL of L15 medium followed by addition of L15 medium (20 µL) containing [^{3}H]**5** (10-fold concentrated). To determine the unspecific binding and the effect of a compound of interest on the equilibrium binding [^{3}H]**5**, the wells were filled with 160 µL of L15 medium followed by addition of L15 medium (20 µL) containing **6** or the compound of interest (10-fold concentrated) and L15 medium (20 µL) containing [^{3}H]**5** (10-fold concentrated).

Saturation binding with [^{3}H]**44** and [^{3}H]**64** at intact CHO-hM_2R cells was performed in the same manner as saturation-binding experiments with [^{3}H]**5**[22] with minor modifications: unspecific binding was determined in the presence of **6** (500-fold excess to [^{3}H]**44** or [^{3}H]**64**), and the incubation period was 2 h.

Saturation and equilibrium competition-binding experiments with [^{3}H]**44** and [^{3}H]**64** at CHO-hM_2R cell homogenates were performed according to the procedure described for saturation and competition-binding experiments with [^{3}H]**19** at CHO-hM_2R cell homogenates,[23] using a total volume per well of 200 instead of 100 µL. The total amount of soluble protein per well was between 19 and 43 µg. In the case of competition-binding experiments, the radioligand concentration was 2.0 and 0.3 nM, respectively. To keep the total volume per well at 200 µL in the case of saturation-binding experiments performed with [^{3}H]**64** in the presence of **14**, the addition of L15 medium (20 µL) containing **14** (10-fold concentrated) was compensated by an equivalent reduction in the volume of L15 medium added to the wells.

M_2R association experiments with [^{3}H]**44** and [^{3}H]**64** were performed at CHO-hM_2R cell homogenates essentially using the procedure described for saturation-binding experiments with [^{3}H]**19** at CHO-hM_2R cell homogenates.[23] The radioligand concentration was 2 and 0.6 nM, respectively. The incubation was started in reversed order after different periods of time (120−1 min). After last addition of the radioligand, homogenates were collected on filter mats using the Harvester. Unspecific binding was determined in the presence of **6** (500-fold excess to the radioligand). For M_2R dissociation experiments with [^{3}H]**44** and [^{3}H]**64**, performed at CHO-hM_2R cell homogenates, the procedure was essentially the same as for saturation-binding experiments with [^{3}H]**19** at CHO-hM_2R cell homogenates.[23] The preincubation (60 min) of the cell homogenates with the radioligand ([^{3}H]**44**: 4 nM, [^{3}H]**64**: 0.6 nM) was started in reversed order after different periods of time ([^{3}H]**44**: between 180 and 1 min and [^{3}H]**64**: between 150 and 1 min) by addition of L15 medium (10 µL) containing the radioligand (10-fold concentrated) to the wells preloaded with L15 medium (80 µL) and cell homogenates (10 µL). The dissociation was started by addition of 10 µL of L15 medium containing **6** (40 and 6 µM, respectively) and was stopped by collection and washing of the homogenates using the harvester. To determine unspecific binding, **6** (1000-fold excess to the radioligand) was added during the preincubation step.

4.7. Data Processing. Retention (capacity) factors were calculated from retention times (t_R) according to $k = (t_R - t_0)/t_0$ (t_0 = dead time). Data from the IP1 accumulation assay and radioligand-binding assays [saturation binding (including Schild-like analysis), association and dissociation kinetics, and equilibrium competition binding] were processed as described previously.[23] Statistical significance (curve slopes) was assessed by a t-test (one-sample, two-tailed). Propagated errors were calculated according to the Gaussian law of errors.

DOI: 10.1021/acsomega.7b01085
ACS Omega 2017, 2, 6741−6754

■ ASSOCIATED CONTENT

Supporting Information

The Supporting Information is available free of charge on the ACS Publications website at DOI: 10.1021/acsomega.7b01085.

Description of the synthesis of intermediates **20**, **21**, **23**, **26**, **30**, **32**, **33**, **36**, **37**, **40**, **42**, **45**, **47**, **49**, **53**, **55–57**, **62**, **65**, **68**, and **71**; experimental protocols for the synthesis and analytical data of compounds **20–23**, **25**, **26–39**, **43–57**, **58–72**, **75–77**, **79–81**, **83**, **84**, **86**, **87**, **89**, **90**, **92**, **93**, **95–97**, **100–104**, **108–110**, **114–116**, **119**, **121**, **122**, and **124**; experimental protocol for the synthesis of the radioligands [^{3}H]**44** and [^{3}H]**64**; ^{1}H-NMR and ^{13}C-NMR spectra of compounds **22**, **25**, **27–29**, **31**, **34**, **35**, **38**, **39**, **43**, **44**, **46**, **48**, **50–52**, **55**, **58–61**, **63**, **64**, **66**, **67**, **69**, **70**, and **72**; RP-HPLC chromatograms of compounds **22**, **25**, **27–29**, **31**, **34**, **35**, **38**, **39**, **43**, **44**, **46**, **48**, **50–52**, **55**, **58–61**, **63**, **64**, **66**, **67**, **69**, **70**, and **72** (PDF)

■ AUTHOR INFORMATION

Corresponding Author

*E-mail: max.keller@ur.de. Phone: (+49)941-9433329. Fax: (+49)941-9434820 (M.K.).

ORCID

Peter Gmeiner: 0000-0002-4127-197X

Max Keller: 0000-0002-8095-8627

Present Addresses

§HitGen, F7-10, Building B3, Tianfu Life Science Park 88 South Keyuan Road, Chengdu, 610041, China (X.S.).

‖Institute of Organic Chemistry, Faculty of Chemistry and Pharmacy, University of Regensburg, Universitätsstr. 31, D-93053 Regensburg, Germany (J.M.).

Notes

The authors declare no competing financial interest.

■ ACKNOWLEDGMENTS

The authors thank Brigitte Wenzl, Maria Beer-Krön, Dita Fritsch, and Susanne Bollwein for excellent technical assistance. The authors also thank Armin Buschauer for providing laboratory equipment and for helpful suggestions. This work was funded by the Graduate Training Program (Graduiertenkolleg) GRK1910 of the Deutsche Forschungsgemeinschaft (DFG) and by the China Scholarship Council (CSC).

■ ABBREVIATIONS

ACh, acetylcholine; Boc, *tert*-butoxycarbonyl; B_{max}, maximum number of binding sites; brs, broad singlet; CH_2Cl_2, dichloromethane; MeCN, acetonitrile; CHO-cells, Chinese hamster ovary cells; DCC, *N,N*′-dicyclohexylcarbodiimide; DIPEA, diisopropylethylamine; DMAP, 4-dimethylaminopyridine; dpm, disintegrations per minute; EtOAc, ethylacetate; GPCR, G-protein coupled receptor; HOBt, 1-hydroxybenzotriazole hydrate; IP1, inositol monophosphate; k, retention (or capacity) factor (HPLC); K_d, dissociation constant obtained from a saturation binding experiment; K_i, dissociation constant obtained from a competition binding experiment; k_{obs}, observed rate constant; k_{off}, dissociation rate constant; k_{on}, association rate constant; MR, muscarinic receptor; M_xR, muscarinic M_x (x = 1–5) receptor; PBS, phosphate buffered saline; pK_b, negative logarithm of the K_b (dissociation constant obtained from a functional assay (inhibition of the effect elicited by an agonist)) in M; pK_i, negative logarithm of the K_i in M; SEM, standard error of the mean; TBTU, 2-(1*H*-benzotriazole-1-yl)-1,1,3,3-tetramethylaminium; TFA, trifluoroacetic acid; t_R, retention time

■ REFERENCES

(1) Hammer, R.; Berrie, C. P.; Birdsall, N. J. M.; Burgen, A. S. V.; Hulme, E. C. Pirenzepine distinguishes between different subclasses of muscarinic receptors. *Nature* **1980**, *283*, 90–92.

(2) Bonner, T.; Buckley, N.; Young, A.; Brann, M. Identification of a family of muscarinic acetylcholine receptor genes. *Science* **1987**, *237*, 527–532.

(3) Caulfield, M. P. Muscarinic receptors—characterization, coupling and function. *Pharmacol. Ther.* **1993**, *58*, 319–379.

(4) Caulfield, M. P.; Birdsall, N. J. International Union of Pharmacology. XVII. Classification of muscarinic acetylcholine receptors. *Pharmacol. Rev.* **1998**, *50*, 279–290.

(5) Lanzafame, A. A.; Christopoulos, A.; Mitchelson, F. Cellular Signaling Mechanisms for Muscarinic Acetylcholine Receptors. *Recept. Channels* **2003**, *9*, 241–260.

(6) Dean, B.; Bymaster, F.; Scarr, E. Muscarinic receptors in schizophrenia. *Curr. Mol. Med.* **2003**, *3*, 419–426.

(7) Clader, J.; Wang, Y. Muscarinic receptor agonists and antagonists in the treatment of Alzheimer's disease. *Curr. Pharm. Des.* **2005**, *11*, 3353–3361.

(8) Haga, K.; Kruse, A. C.; Asada, H.; Yurugi-Kobayashi, T.; Shiroishi, M.; Zhang, C.; Weis, W. I.; Okada, T.; Kobilka, B. K.; Haga, T.; Kobayashi, T. Structure of the human M_2 muscarinic acetylcholine receptor bound to an antagonist. *Nature* **2012**, *482*, 547–551.

(9) Kruse, A. C.; Hu, J.; Pan, A. C.; Arlow, D. H.; Rosenbaum, D. M.; Rosemond, E.; Green, H. F.; Liu, T.; Chae, P. S.; Dror, R. O.; Shaw, D. E.; Weis, W. I.; Wess, J.; Kobilka, B. K. Structure and dynamics of the M_3 muscarinic acetylcholine receptor. *Nature* **2012**, *482*, 552–556.

(10) Thal, D. M.; Sun, B.; Feng, D.; Nawaratne, V.; Leach, K.; Felder, C. C.; Bures, M. G.; Evans, D. A.; Weis, W. I.; Bachhawat, P.; Kobilka, T. S.; Sexton, P. M.; Kobilka, B. K.; Christopoulos, A. Crystal structures of the M_1 and M_4 muscarinic acetylcholine receptors. *Nature* **2016**, *531*, 335–340.

(11) Eglen, R. M.; Choppin, A.; Watson, N. Therapeutic opportunities from muscarinic receptor research. *Trends Pharmacol. Sci.* **2001**, *22*, 409–414.

(12) Mohr, K.; Tränkle, C.; Holzgrabe, U. Structure/activity relationships of M_2 muscarinic allosteric modulators. *Recept. Channels* **2003**, *9*, 229–240.

(13) Voigtländer, U.; Jöhren, K.; Mohr, M.; Raasch, A.; Tränkle, C.; Buller, S.; Ellis, J.; Höltje, H.-D.; Mohr, K. Allosteric site on muscarinic acetylcholine receptors: identification of two amino acids in the muscarinic M_2 receptor that account entirely for the M2/M5 subtype selectivities of some structurally diverse allosteric ligands in N-methylscopolamine-occupied receptors. *Mol. Pharmacol.* **2003**, *64*, 21–31.

(14) Wess, J. Allosteric binding sites on muscarinic acetylcholine receptors. *Mol. Pharmacol.* **2005**, *68*, 1506–1509.

(15) Presland, J. Identifying novel modulators of G protein-coupled receptors via interaction at allosteric sites. *Curr. Opin. Drug Discovery Dev.* **2005**, *8*, 567–576.

(16) Conn, P. J.; Christopoulos, A.; Lindsley, C. W. Allosteric modulators of GPCRs: a novel approach for the treatment of CNS disorders. *Nat. Rev. Drug Discovery* **2009**, *8*, 41–54.

(17) Kruse, A. C.; Ring, A. M.; Manglik, A.; Hu, J.; Hu, K.; Eitel, K.; Hübner, H.; Pardon, E.; Valant, C.; Sexton, P. M. Activation and allosteric modulation of a muscarinic acetylcholine receptor. *Nature* **2013**, *504*, 101–106.

(18) Lüllmann, H.; Ohnesorge, F. K.; Schauwecker, G.-C.; Wassermann, O. Inhibition of the actions of carbachol and DFP on guinea pig isolated atria by alkane-bis-ammonium compounds. *Eur. J. Pharmacol.* **1969**, *6*, 241–247.

DOI: 10.1021/acsomega.7b01085
ACS Omega 2017, 2, 6741–6754

(19) Mohr, K.; Tränkle, C.; Kostenis, E.; Barocelli, E.; De Amici, M.; Holzgrabe, U. Rational design of dualsteric GPCR ligands: quests and promise. *Br. J. Pharmacol.* **2010**, *159*, 997−1008.
(20) Clark, A. L.; Mitchelson, F. The inhibitory effect of gallamine on muscarinic receptors. *Br. J. Pharmacol.* **1976**, *58*, 323−331.
(21) Tränkle, C.; Andresen, I.; Lambrecht, G.; Mohr, K. M_2 receptor binding of the selective antagonist AF-DX 384: possible involvement of the common allosteric site. *Mol. Pharmacol.* **1998**, *53*, 304−312.
(22) Keller, M.; Tränkle, C.; She, X.; Pegoli, A.; Bernhardt, G.; Buschauer, A.; Read, R. W. M_2 Subtype preferring dibenzodiazepinone-type muscarinic receptor ligands: Effect of chemical homo-dimerization on orthosteric (and allosteric?) binding. *Bioorg. Med. Chem.* **2015**, *23*, 3970−3990.
(23) Pegoli, A.; She, X.; Wifling, D.; Hübner, H.; Bernhardt, G.; Gmeiner, P.; Keller, M. Radiolabeled Dibenzodiazepinone-Type Antagonists Give Evidence of Dualsteric Binding at the M_2 Muscarinic Acetylcholine Receptor. *J. Med. Chem.* **2017**, *60*, 3314−3334.
(24) Croy, C. H.; Schober, D. A.; Xiao, H.; Quets, A.; Christopoulos, A.; Felder, C. C. Characterization of the novel positive allosteric modulator, LY2119620, at the muscarinic M_2 and M_4 receptors. *Mol. Pharmacol.* **2014**, *86*, 106−115.
(25) Schober, D. A.; Croy, C. H.; Xiao, H.; Christopoulos, A.; Felder, C. C. Development of a Radioligand, [^{3}H]LY2119620, to Probe the Human M_2 and M_4 Muscarinic Receptor Allosteric Binding Sites. *Mol. Pharmacol.* **2014**, *86*, 116−123.
(26) Shonberg, J.; Scammells, P. J.; Capuano, B. Design strategies for bivalent ligands targeting GPCRs. *ChemMedChem* **2011**, *6*, 963−974.
(27) Berque-Bestel, I.; Lezoualc'h, F.; Jockers, R. Bivalent ligands as specific pharmacological tools for G protein-coupled receptor dimers. *Curr. Drug Discovery Technol.* **2008**, *5*, 312−318.
(28) Bhushan, R. G.; Sharma, S. K.; Xie, Z.; Daniels, D. J.; Portoghese, P. S. A bivalent ligand (KDN-21) reveals spinal δ and κ opioid receptors are organized as heterodimers that give rise to δ_1 and κ_2 phenotypes. Selective targeting of $\delta-\kappa$ heterodimers. *J. Med. Chem.* **2004**, *47*, 2969−2972.
(29) Birnkammer, T.; Spickenreither, A.; Brunskole, I.; Lopuch, M.; Kagermeier, N.; Bernhardt, G.; Dove, S.; Seifert, R.; Elz, S.; Buschauer, A. The bivalent ligand approach leads to highly potent and selective acylguanidine-type histamine H_2 receptor agonists. *J. Med. Chem.* **2012**, *55*, 1147−1160.
(30) Kagermeier, N.; Werner, K.; Keller, M.; Baumeister, P.; Bernhardt, G.; Seifert, R.; Buschauer, A. Dimeric carbamoylguanidine-type histamine H_2 receptor ligands: A new class of potent and selective agonists. *Bioorg. Med. Chem.* **2015**, *23*, 3957−3969.
(31) Huber, D.; Hübner, H.; Gmeiner, P. 1,1′-Disubstituted ferrocenes as molecular hinges in mono- and bivalent dopamine receptor ligands. *J. Med. Chem.* **2009**, *52*, 6860−6870.
(32) Kühhorn, J.; Hübner, H.; Gmeiner, P. Bivalent dopamine D_2 receptor ligands: synthesis and binding properties. *J. Med. Chem.* **2011**, *54*, 4896−4903.
(33) Soriano, A.; Ventura, R.; Molero, A.; Hoen, R.; Casadó, V.; Cortés, A.; Fanelli, F.; Albericio, F.; Lluís, C.; Franco, R.; Royo, M. Adenosine A_2A receptor-antagonist/dopamine D_2 receptor-agonist bivalent ligands as pharmacological tools to detect A_2A-D_2 receptor heteromers. *J. Med. Chem.* **2009**, *52*, 5590−5602.
(34) Jacobson, K. A.; Xie, R.; Young, L.; Chang, L.; Liang, B. T. A novel pharmacological approach to treating cardiac ischemia binary conjugates of A_1 and A_3 adenosine receptor agonists. *J. Biol. Chem.* **2000**, *275*, 30272−30279.
(35) Hausler, N. E.; Devine, S. M.; McRobb, F. M.; Warfe, L.; Pouton, C. W.; Haynes, J. M.; Bottle, S. E.; White, P. J.; Scammells, P. J. Synthesis and pharmacological evaluation of dual acting antioxidant A_{2A} adenosine receptor agonists. *J. Med. Chem.* **2012**, *55*, 3521−3534.
(36) Weiss, S.; Keller, M.; Bernhardt, G.; Buschauer, A.; König, B. Modular synthesis of non-peptidic bivalent NPY Y_1 receptor antagonists. *Bioorg. Med. Chem.* **2008**, *16*, 9858−9866.
(37) Keller, M.; Teng, S.; Bernhardt, G.; Buschauer, A. Bivalent Argininamide-Type Neuropeptide Y Y_1 Antagonists Do Not Support the Hypothesis of Receptor Dimerisation. *ChemMedChem* **2009**, *4*, 1733−1745.
(38) Keller, M.; Kaske, M.; Holzammer, T.; Bernhardt, G.; Buschauer, A. Dimeric argininamide-type neuropeptide Y receptor antagonists: chiral discrimination between Y_1 and Y_4 receptors. *Bioorg. Med. Chem.* **2013**, *21*, 6303−6322.
(39) Davie, B. J.; Christopoulos, A.; Scammells, P. J. Development of M_1 mAChR allosteric and bitopic ligands: prospective therapeutics for the treatment of cognitive deficits. *ACS Chem. Neurosci.* **2013**, *4*, 1026−1048.
(40) Valant, C.; Lane, J. R.; Sexton, P. M.; Christopoulos, A. The best of both worlds? Bitopic orthosteric/allosteric ligands of g protein−coupled receptors. *Annu. Rev. Pharmacol. Toxicol.* **2012**, *52*, 153−178.
(41) Antony, J.; Kellershohn, K.; Mohr-Andra, M.; Kebig, A.; Prilla, S.; Muth, M.; Heller, E.; Disingrini, T.; Dallanoce, C.; Bertoni, S.; Schrobang, J.; Tränkle, C.; Kostenis, E.; Christopoulos, A.; Holtje, H.-D.; Barocelli, E.; De Amici, M.; Holzgrabe, U.; Mohr, K. Dualsteric GPCR targeting: a novel route to binding and signaling pathway selectivity. *FASEB J.* **2009**, *23*, 442−450.
(42) Lane, J. R.; Sexton, P. M.; Christopoulos, A. Bridging the gap: bitopic ligands of G-protein-coupled receptors. *Trends Pharmacol. Sci.* **2013**, *34*, 59−66.
(43) Disingrini, T.; Muth, M.; Dallanoce, C.; Barocelli, E.; Bertoni, S.; Kellershohn, K.; Mohr, K.; De Amici, M.; Holzgrabe, U. Design, synthesis, and action of oxotremorine-related hybrid-type allosteric modulators of muscarinic acetylcholine receptors. *J. Med. Chem.* **2006**, *49*, 366−372.
(44) Steinfeld, T.; Mammen, M.; Smith, J. A. M.; Wilson, R. D.; Jasper, J. R. A novel multivalent ligand that bridges the allosteric and orthosteric binding sites of the M_2 muscarinic receptor. *Mol. Pharmacol.* **2007**, *72*, 291−302.
(45) Dörje, F.; Wess, J.; Lambrecht, G.; Tacke, R.; Mutschler, E.; Brann, M. R. Antagonist binding profiles of five cloned human muscarinic receptor subtypes. *J. Pharmacol. Exp. Ther.* **1991**, *256*, 727−733.
(46) Gitler, M. S.; Reba, R. C.; Cohen, V. I.; Rzeszotarski, W. J.; Baumgold, J. A novel m2-selective muscarinic antagonist: binding characteristics and autoradiographic distribution in rat brain. *Brain Res.* **1992**, *582*, 253−260.
(47) Mohr, M.; Heller, E.; Ataie, A.; Mohr, K.; Holzgrabe, U. Development of a new type of allosteric modulator of muscarinic receptors: hybrids of the antagonist AF-DX 384 and the hexamethonio derivative W84. *J. Med. Chem.* **2004**, *47*, 3324−3327.
(48) Holzgrabe, U.; De Amici, M.; Mohr, K. Allosteric modulators and selective agonists of muscarinic receptors. *J. Mol. Neurosci.* **2006**, *30*, 165−167.
(49) Shekhar, A.; Potter, W. Z.; Lightfoot, J.; Lienemann, J.; Dubé, S.; Mallinckrodt, C.; Bymaster, F. P.; McKinzie, D. L.; Felder, C. C. Selective muscarinic receptor agonist xanomeline as a novel treatment approach for schizophrenia. *Am. J. Psychiatry* **2008**, *165*, 1033−1039.
(50) Bridges, T. M.; Brady, A. E.; Kennedy, J. P.; Daniels, R. N.; Miller, N. R.; Kim, K.; Breininger, M. L.; Gentry, P. R.; Brogan, J. T.; Jones, C. K.; Conn, P. J.; Lindsley, C. W. Synthesis and SAR of analogues of the M_1 allosteric agonist TBPB. Part I: Exploration of alternative benzyl and privileged structure moieties. *Bioorg. Med. Chem. Lett.* **2008**, *18*, 5439−5442.
(51) Miller, N. R.; Daniels, R. N.; Bridges, T. M.; Brady, A. E.; Conn, P. J.; Lindsley, C. W. Synthesis and SAR of analogs of the M_1 allosteric agonist TBPB. Part II: Amides, sulfonamides and ureas—The effect of capping the distal basic piperidine nitrogen. *Bioorg. Med. Chem. Lett.* **2008**, *18*, 5443−5447.
(52) Jones, C. K.; Brady, A. E.; Davis, A. A.; Xiang, Z.; Bubser, M.; Tantawy, M. N.; Kane, A. S.; Bridges, T. M.; Kennedy, J. P.; Bradley, S. R. Novel selective allosteric activator of the M_1 muscarinic acetylcholine receptor regulates amyloid processing and produces antipsychotic-like activity in rats. *J. Neurosci.* **2008**, *28*, 10422−10433.
(53) Keov, P.; Valant, C.; Devine, S. M.; Lane, J. R.; Scammells, P. J.; Sexton, P. M.; Christopoulos, A. Reverse engineering of the selective agonist TBPB unveils both orthosteric and allosteric modes of action

DOI: 10.1021/acsomega.7b01085
ACS Omega 2017, 2, 6741−6754

at the M_1 muscarinic acetylcholine receptor. *Mol. Pharmacol.* **2013**, *84*, 425–437.

(54) Avlani, V. A.; Langmead, C. J.; Guida, E.; Wood, M. D.; Tehan, B. G.; Herdon, H. J.; Watson, J. M.; Sexton, P. M.; Christopoulos, A. Orthosteric and allosteric modes of interaction of novel selective agonists of the M_1 muscarinic acetylcholine receptor. *Mol. Pharmacol.* **2010**, *78*, 94–104.

(55) Huang, F.; Buchwald, P.; Browne, C. E.; Farag, H. H.; Wu, W.-M.; Ji, F.; Hochhaus, G.; Bodor, N. Receptor binding studies of soft anticholinergic agents. *AAPS PharmSci* **2001**, *3*, 44–56.

(56) Maggio, R.; Barbier, P.; Bolognesi, M. L.; Minarini, A.; Tedeschi, D.; Melchiorre, C. Binding profile of the selective muscarinic receptor antagonist tripitramine. *Eur. J. Pharmacol.* **1994**, *268*, 459–462.

(57) Copeland, R. A. Conformational adaptation in drug–target interactions and residence time. *Future Med. Chem.* **2011**, *3*, 1491–1501.

(58) Vauquelin, G. Simplified models for heterobivalent ligand binding: when are they applicable and which are the factors that affect their target residence time. *Naunyn-Schmiedeberg's Arch. Pharmacol.* **2013**, *386*, 949–962.

(59) Tränkle, C.; Weyand, O.; Voigtländer, U.; Mynett, A.; Lazareno, S.; Birdsall, N. J. M.; Mohr, K. Interactions of orthosteric and allosteric ligands with [^{3}H]dimethyl-W84 at the common allosteric site of muscarinic M_2 receptors. *Mol. Pharmacol.* **2003**, *64*, 180–190.

(60) Keller, M.; Pop, N.; Hutzler, C.; Beck-Sickinger, A. G.; Bernhardt, G.; Buschauer, A. Guanidine–acylguanidine bioisosteric approach in the design of radioligands: synthesis of a tritium-labeled N^G-propionylargininamide ([3H]-UR-MK114) as a highly potent and selective neuropeptide Y Y1 receptor antagonist. *J. Med. Chem.* **2008**, *51*, 8168–8172.

(61) Kane, B. E.; Grant, M. K. O.; El-Fakahany, E. E.; Ferguson, D. M. Synthesis and evaluation of xanomeline analogs—Probing the wash-resistant phenomenon at the M_1 muscarinic acetylcholine receptor. *Bioorg. Med. Chem.* **2008**, *16*, 1376–1392.

(62) Cohen, V. I.; Baumgold, J.; Jin, B.; De la Cruz, R.; Rzeszotarski, W. J.; Reba, R. C. Synthesis and structure-activity relationship of some 5-[[[(dialkylamino)alkyl]-1-piperidinyl]acetyl]-10,11-dihydro-5H-dibenzo[b,e][1,4]diazepin-11-ones as M_2-selective antimuscarinics. *J. Med. Chem.* **1993**, *36*, 162–165.

DOI: 10.1021/acsomega.7b01085
ACS Omega 2017, 2, 6741–6754